Porosity Reduction During Diagenesis of Diatomaceous Rocks[1]

Caren Chaika[2] and Jack Dvorkin[3]

ABSTRACT

With lithification and burial, diatomaceous rock transforms from opal-A to opal-CT and then quartz. This study documents two different patterns of porosity reduction and their associated mineralogical and density changes using samples from the Monterey Formation, California. Samples that have one set of properties are called group 1, and those showing other trends are assigned to group 2.

In one pattern, the samples (group 1) exhibit gradual porosity change with the opal-A/opal-CT transition. Opal-A and opal-CT coexist in the same samples, and samples bearing only opal-A or only opal-CT may have similar porosities. In the other pattern (group 2), the opal-A/opal-CT transition is associated with a sharp decrease in porosity. In this data set, opal-A and opal-CT are not present within the same sample. Samples bearing only opal-A have porosity above 55%, whereas those with only opal-CT have porosity below 43%.

It appears that the two patterns separate from each other when opal-A dissolves and different minerals precipitate preferentially from the silica in solution. In group 1, the content of clay minerals, particularly illite and smectite, increases as porosity decreases. This suggests that porosity reduction is due to pore filling by authigenic clay minerals. In group 2, the amount of opal-CT or quartz increases with decreasing porosity, and the weight percent of clay minerals also decreases. This implies that porosity reduction occurs predominantly through addition of silica.

Porosity in the opal-CT–bearing samples of group 1 is larger than that of the opal-CT–bearing samples of group 2. This fact has significant implications for exploration in these important oil-bearing rocks.

INTRODUCTION

Far from sources of detrital input, most silica in deep ocean basins precipitates biogenically as diatom and radiolarian frustules. Such biogenic silica is amorphous opal (opal-A), which readily dissolves at the surface and near-surface conditions. As diagenesis progresses, opal-A alters toward quartz, the stable phase, through an intermediate phase, opal-CT. In shallow systems, opal-A dissolves and reprecipitates as interlayers of cristobalite and tridymite (opal-CT) before forming quartz (Murata and Randall, 1975; Rimstidt and Barnes, 1980; Pisciotto, 1981; Williams and Crerar, 1985). Opal-CT gradually becomes more ordered crystallographically (and, therefore, more dense) until it, too, dissolves and then reprecipitates as quartz (Dove and Rimstidt, 1994; Graetsch, 1994).

Grain density in opal-A ranges from 1.9 to 2.2 g/cm^3 and in opal-CT from 2.0 to 2.3 g/cm^3 (L. A. Williams, 1997, personal communication; D. G. Harville, 1997, personal communication; Chaika, 1998). This density is much smaller than that of quartz (2.65 g/cm^3) (Carmichael, 1989). In general, with the change from opal-A to opal-CT, grain density increases by about 0.1 g/cm^3 and porosity may reduce by 20% (Murata and Larson, 1975; Beyer, 1987). Although this change in grain density is small, the porosity reduction results in a significant bulk density change at both diagenetic transitions.

The existence of relationships among porosity, density, and the stage of silica diagenesis are well documented by both laboratory and well log data. For example, O'Brien et al. (1989), Nobes et al.

[1]Manuscript received February 10, 1998; revised manuscript received January 13, 2000; final acceptance February 15, 2000.

[2]Department of Geological and Environmental Sciences, Stanford University, Stanford, California 94305. Present address: Occidental of Elk Hills, P.O. Box 1001, Tupman, California 93276.

[3]Geophysics Department, Stanford University, Stanford, California 94305.

We are thankful to a number of sources for donations of samples and data. Core and associated data from wells at Asphalto, Cymric, and McKittrick were provided by Chevron (Steve Smith, Bruce Bilodeau, and Tom Zalan, among others). Data and core from a well at South Belridge were provided by Mobil (Bob Timmer), and the Core Warehouse at the California State University at Bakersfield provided data and core from a Shell well at North Belridge. Mineralogy, porosity, and density of all San Joaquin Valley samples were measured at Core Lab in Bakersfield, California. The Stanford Rock Physics Laboratory provided facilities for supplementary core measurements. Steve Graham and Loretta Williams gave important inputs to our understanding of the processes discussed. Reviews by Raymond Siever, Salman Block, and an anonymous reviewer greatly improved the clarity of the manuscript. The work was supported by the American Chemical Society Petroleum Research Fund Grant ACS-PRF no. 32743-AC2 and by Norsk Hydro.

(1992), and Guerin and Goldberg (1996) correlated the opal-A/opal-CT and opal-CT/quartz transitions in Deep-Sea Drilling Project (DSDP) wells to changes in porosity, bulk density, and acoustic velocity. Beyer (1987), O'Brien et al. (1989), and Tribble et al. (1992) documented well-pronounced relationships between the stage of silica diagenesis and bulk density and porosity from core measurements.

This study is based on porosity, density, and mineralogy measurements from the Monterey Formation, California. This unit is of considerable interest to the petroleum industry because it is a major hydrocarbon source and reservoir rock. Our work shows that two distinctively different patterns of porosity reduction exist in these rocks. Porosity reduction in the first pattern (group 1) is caused by pore-filling of nonsilica minerals. These rocks exhibit a gradual porosity decrease between rocks containing opal-A and opal-CT. Porosity reduction in the second pattern (group 2) is controlled by the silica component, and these rocks are easily identified by a porosity gap between rocks bearing opal-A and opal-CT.

The results presented here are based on core data from five oil fields in the southwest San Joaquin Valley and outcrop samples (Compton, 1991) collected near Point Pedernales, California (Figure 1). The samples from Cymric, North Belridge, South Belridge, and Point Pedernales traverse the opal-A/opal-CT transition, those from McKittrick are all opal-CT–bearing, and those from Asphalto traverse the opal-CT/quartz transition.

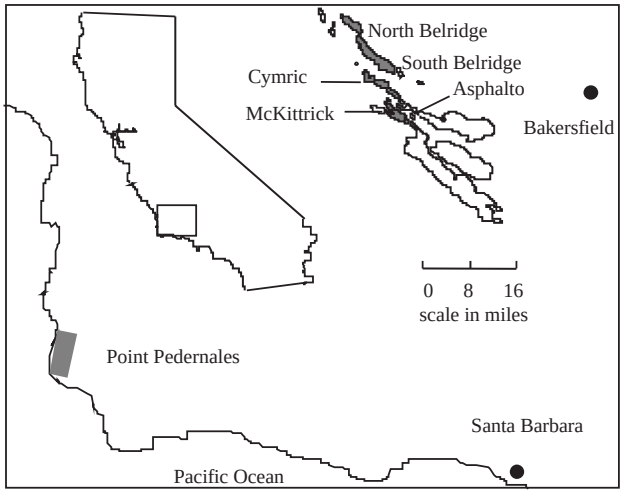

Figure 1—Sample locations.

METHODOLOGY

The weight percent of the minerals in all of the San Joaquin Valley samples was determined with Fourier transform infrared spectroscopy (FTIR), as discussed by Harville and Freeman (1988). Weight percents of different minerals are reproducible within 5%. Because large amounts of opal-A and opal-CT were present in most samples, the speed and reliability of FTIR made it arguably the best single method to determine mineralogic content in these samples (e.g., Rice et al., 1995).

These oil field data are supplemented with data published in Compton (1991). He determined mineralogy using a combination of x-ray diffraction (XRD), elemental analyses, and organic carbon analyses. Supplemental analyses included x-ray fluorescence (XRF), petrography, and scanning electron microscopy (SEM) to determine the weight fractions of the different constituent minerals.

Although the measurements of mineralogic content between the Point Pedernales rocks and the others were performed in different laboratories using different methods, they have similar high levels of accuracy and so can legitimately be compared to each other. Porosity and grain density were measured directly in all samples. Dry bulk density (ρ_b) was calculated from porosity (ϕ) and grain density (ρ_s) as $\rho_b = \rho_s(1 - \phi)$.

In the San Joaquin Valley samples, the weight of the matrix was determined after all pore fluids were extracted, and both grain volume and porosity were determined using Boyle's law and helium as the gaseous medium. Pore fluids were removed by Core Laboratories, Inc., by cleaning the samples with boiling toluene at approximately 115°C and then removing the remainder of the oil with methylene chloride, which boils at about 45°C. All samples were dried in either a humidity-controlled oven or a convection oven at approximately 115°C for between 4 and 48 hr. FTIR analyses show that waters of hydration remain bound to both opal and clay minerals. After preparation, all samples were kept room dry. Bulk density was also measured directly in 24 San Joaquin Valley samples and is consistent with calculated data within a range of 0.01 to 0.08 g/cm^3 for 22 out of the 24 samples, with the two outliers at a difference of 0.14–0.15 g/cm^3.

Porosity and grain density of the Point Pedernales samples were measured by weighing the samples both before and after being vacuum impregnated with toluene, and the volume was determined by comparing the latter weight to the weight of the sample while it was immersed in toluene. The initial, dry weight was made after the samples were dried overnight at 105°C. Compton (1991) reported that his porosity measurements are repeatable within 0.5%.

All data sets were restricted to samples in which the silica content exceeded 40% (thus, the porosity and density of several samples in the Point Pedernales data set that lack mineralogic information are omitted from this analysis). Most of the samples eliminated from the study are high in carbonates; their removal permits this study to focus on physical property variations that occur due to silica diagenesis. The data used in this study are shown in the Appendix.

TWO POROSITY REDUCTION PATTERNS

Plots of dry-rock bulk density ρ_b vs. porosity ϕ produce two distinctive linear trends (Figure 2A):

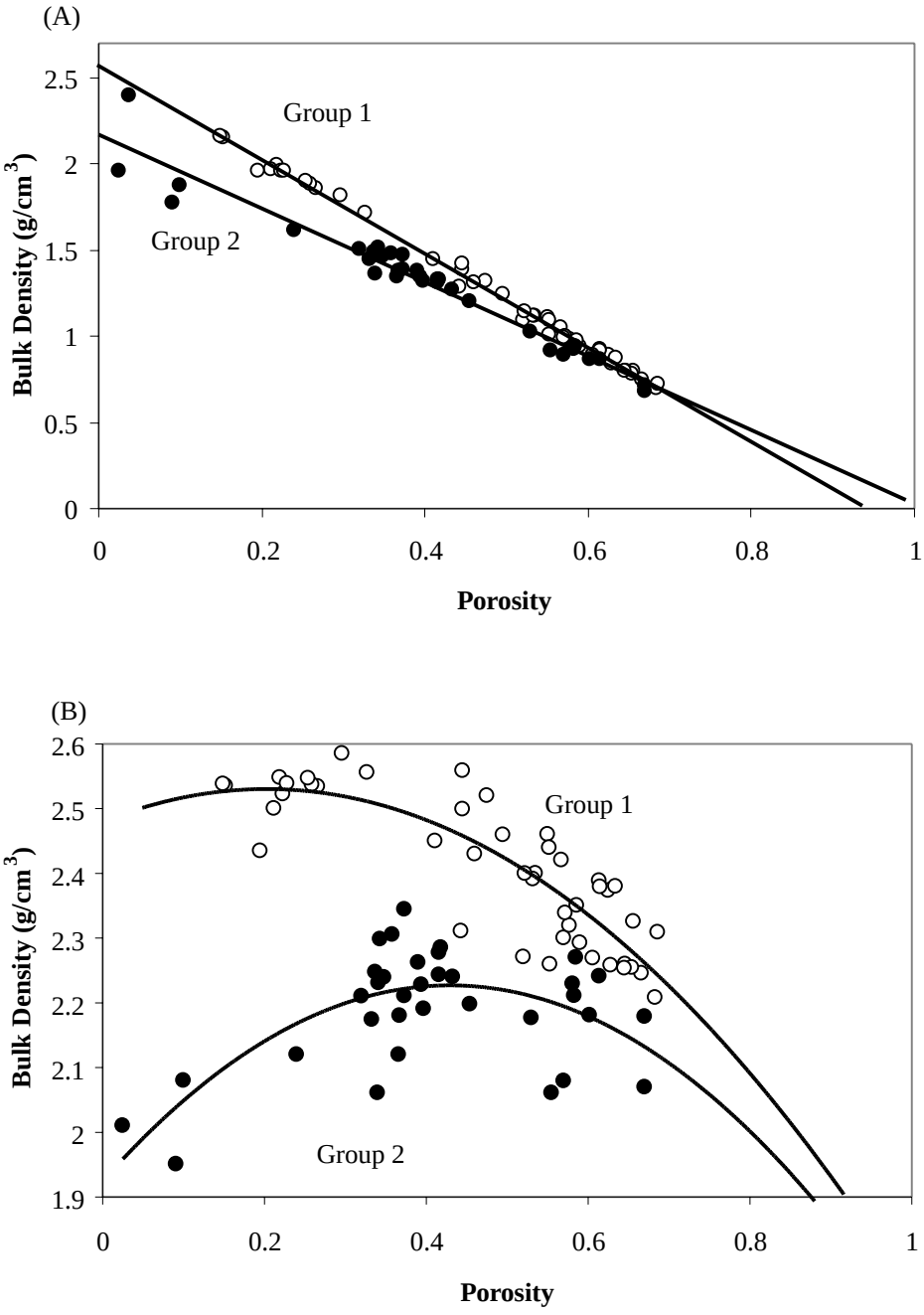

Figure 2—Dry-rock bulk density (A) and grain density (B) vs. porosity. Open symbols represent the Belridge, Cymric, and Asphalto samples (group 1), and filled symbols represent the Point Pedernales and McKittrick samples (group 2).

$$\rho_b = 2.573 - 2.727\phi$$
$$R^2 = 0.995 \quad (1)$$
$$n = 45$$

and

$$\rho_b = 2.174 - 2.142\phi$$
$$R^2 = 0.950 \quad (2)$$
$$n = 35$$

where density is in grams per cubic centimeter, porosity is a volume fraction, R^2 is the correlation coefficient, and n is the number of samples. Regression 1 describes the samples from Belridge, Cymric, and Asphalto, and regression 2 describes those from Point Pedernales and McKittrick. The high correlation coefficients mean that the porosity variations almost entirely describe the variation in dry bulk density. The samples in the trends described by regressions 1 and 2 are group 1 and 2, respectively.

The only quartz-bearing group 2 sample is an outlier that plots with the group 1 samples. Thus, although the change in bulk density through the opal-A/ opal-CT transition is described by the linear trend, changes associated with the opal-CT to quartz transition most likely are not. Because there is only one group 2 sample where most silica is in the form of quartz, the opal-CT/quartz transition cannot be discussed for group 2 samples, and this data point will be removed from successive graphs unless noted.

We have already noted that the grain density of silica increases as it alters from opal-A to opal-CT to quartz; therefore, it is expected that grain density of the samples will increase with porosity reduction and silica diagenesis. Plots of grain density vs. porosity produce the trends (Figure 2B):

$$\rho_s = 2.479 + 0.498\phi - 1.230\phi^2$$
$$R^2 = 0.721 \quad (3)$$
$$n = 45$$

for the samples in group 1 and

$$\rho_s = 1.925 + 1.409\phi - 1.641\phi^2$$
$$R^2 = 0.457 \quad (4)$$
$$n = 34$$

for the samples in group 2.

Figure 2B shows that grain density increases with porosity reduction in the group 1 samples fit by equation 3. In contrast, grain density decreases slightly with porosity reduction in the group 2 samples described by equation 4. The low correlation coefficients of equations 3 and 4 mean that porosity variations explain only part of the change in grain density.

The two trends are caused by the difference in grain density between low-density opal-A and opal-CT vs. the other, higher density components. The grain densities of opal-A and opal-CT are both much lower than any of the other significant (>5%) minerals in these samples, with densities that range from 2.56 to 2.71 g/cm^3 (orthoclase feldspar to calcite) (Zoltai and Stout, 1984); therefore, if the fraction of opal-A and/or opal-CT decreases, then the fraction of quartz and nonsilica minerals must increase, and the grain density of the whole rock increases. Similarly, if the fraction of opal-A or opal-CT increases with porosity reduction, then there must be a smaller fraction of higher density nonsilica minerals (or quartz, if present), and the grain density of the rock will decrease. These two variations explain the group 1 and group 2 trends, respectively.

A decrease in grain density with porosity reduction such as that shown by the group 2 samples in Figure 2B is unusual enough to warrant more proof that compositional changes are responsible for this trend. Plots of opal-A, opal-CT, and quartz vs. porosity for all samples (including the quartz-phase group 2 sample) show that with decreasing porosity, opal-A and opal-CT decrease in group 1 samples (Figure 3A). In contrast, in group 2 the opal-CT–bearing samples contain more silica than the opal-A–phase samples (Figure 3B); more silica precipitated as opal-CT than was present as opal-A. The quartz in most samples in this study can be assumed to be detrital because it coexists with opal-A and early opal-CT samples; only the quartz in the samples from Asphalto (group 1) and the group 2 sample at a porosity of 0.037 is assumed to be diagenetically altered biogenic silica.

The relationship of silica polymorph to porosity is shown through a regression of opal-A + opal-CT vs. porosity. Opal-A and opal-CT are combined because grain density is relatively constant through the opal-A to opal-CT transition; furthermore, because there is only one quartz-bearing group 2 sample, porosity variations with the opal-CT to quartz transition cannot be compared between the two groups. Because total opal content (opal-A + opal-CT) varies with porosity, opal is the dependent variable in second-order regressions with porosity where

$$\text{Opal A} + \text{Opal CT} = 0.059 - 0.330\phi + 2.030\phi^2$$
$$R^2 = 0.792 \quad (5)$$
$$n = 45$$

in the group 1 samples and

$$\text{Opal A} + \text{Opal CT} = 0.483 + 1.758\phi - 2.879\phi^2$$
$$R^2 = 0.305 \quad (6)$$
$$n = 35$$

in the group 2 samples.

The regressions show that the weight percent of opal-A + opal-CT decreases smoothly through the opal-A/opal-CT transition only in the group 1 samples. It follows that the content of the detrital quartz or nonsilica minerals must be increasing. Because the amount of quartz is roughly constant in Figure 3A, an increase in nonsilica minerals with porosity reduction is responsible for the increase in grain density with decreasing porosity in group 1. This explanation, that porosity decreases due to the increased abundance of nonopaline minerals, was espoused by Schwartz (1988) to explain similar trends in diatomites of the South Belridge field in the San Joaquin Valley.

Mechanical compaction of rock can also act to reduce porosity. For example, smooth changes in porosity and density associated with the opal-A to opal-CT transition and the opal-CT to quartz transition (as seen in the group 1 samples) were observed in siliceous rocks of north Japan by Tada and Iijima (1983), who attributed porosity reduction to compaction.

Although mechanical compaction may play a part in porosity reduction of the high-porosity Cymric samples, it does not play a significant role in the samples from McKittrick or Asphalto. Laboratory ultrasonic velocity experiments (Chaika, 1998) at hydrostatic pressures near or greater than in situ pressure show little change in length of the McKittrick and Asphalto samples; however, significant shortening did occur in the Cymric samples at in situ pressures (6 MPa) (S. Sanford, 1998, personal communication). Unlike the samples from greater depths, the Cymric reservoir is made mostly of opal-A–phase rocks. Thus, porosity reduction does not seem to be caused by mechanical compaction after the silica has undergone the opal-A to opal-CT transition. Instead, porosity decrease in group 1 rocks is associated with a gradual increase in authigenic nonsilica minerals.

In contrast, both the sample data and the low correlation coefficient in equation 6 suggest that porosity reduction in group 2 rocks is associated with an abrupt diagenetic change. The biogenic silica content in the group 2 samples cannot be described by one second-order regression equation as can the group 1 samples. Instead, these rocks show a 25% drop in porosity associated with the opal-A to opal-CT transition; however, it is reasonable to attribute the decrease in grain density with decreasing porosity with the steplike increase in biogenic silica from about 40% to near 100% of the rock at the opal-A/opal-CT transition.

There is another difference between the two data sets: only the group 2 samples have a data gap in the porosity interval from 43 to 50%; furthermore, samples of porosity below 43% contain only the silica polymorph opal-CT, whereas those above 50% porosity contain only opal-A.

This porosity gap has an important corollary: opal-CT–phase rocks can exist at greater porosity in group 1 than group 2 samples. Figure 3A (group 1) shows opal-CT–bearing samples at porosity as great as 68%, and samples where the silica has completely altered from opal-A to opal-CT at porosity of 65%. In contrast, the highest porosity opal-CT–bearing sample in Figure 3B (group 2) has a porosity of 43%, which compares better to previous observations of a maximum porosity of 40% (e.g., Isaacs, 1981). The data from the diagenetic quartz-bearing samples of Asphalto suggest that group 1 quartz-phase rocks also can have greater than expected porosity; these biogenic quartz-phase rocks exist at porosity as great as 44% in opal-CT/quartz mixtures, and at 26% porosity where the opal-CT/quartz transition is complete. In contrast, prior studies suggest that quartz-phase rocks have porosity of less than 20% (Isaacs, 1981).

Because the silica diagenetic transitions in the group 2 samples have a strong effect on porosity reduction, factors that affect these transitions affect porosity, as well.

CLAY MINERALS AND POROSITY REDUCTION PATTERNS

Within a transition zone, silica transformations can be accelerated or retarded due to variations in detrital mineral composition, magnesium-rich clays, and carbonate (Merino, 1975; Kastner et al., 1977; Isaacs, 1983; Williams et al., 1985). Experimental work has shown that clay minerals retard the opal-A to opal-CT transition and accelerate the opal-CT to quartz transition (e.g., Kastner et al., 1977; Hinman, 1990). Clays retard the first transition by preventing opal-A from dissolving. By filling pore space, clay prevents circulating fluids from dissolving opal-A. Because the formation of opal-CT is retarded, it initially forms at greater temperatures and is well ordered crystallographically. This well-ordered opal-CT alters to quartz more quickly (Isaacs, 1983; Williams et al., 1985).

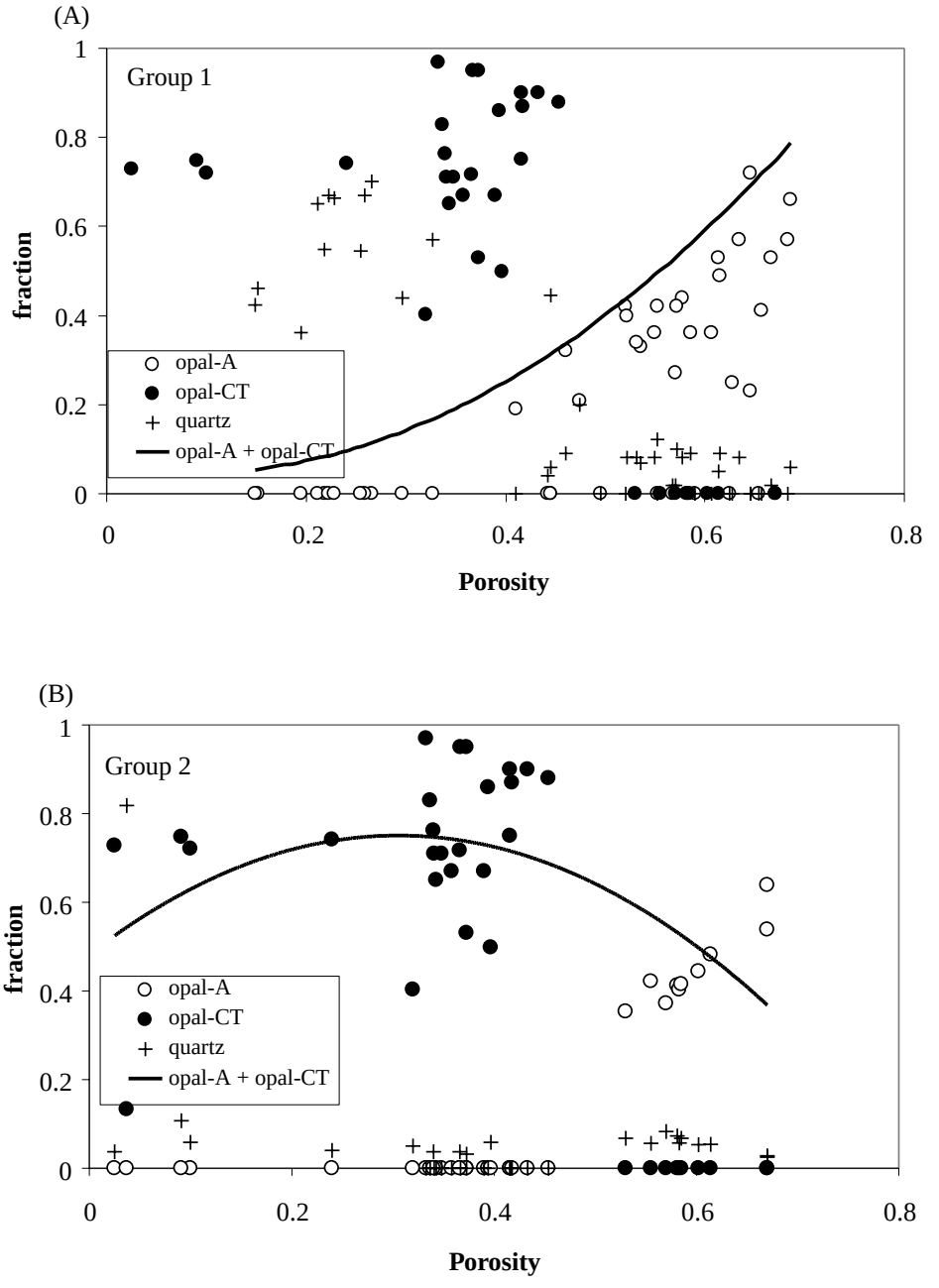

Figure 3—Fraction of opal-A, opal-CT, quartz, and opal-A + opal-CT in (A) group 1 and (B) group 2 samples.

Unfortunately, there is not an easy method to determine if the clay is authigenic or detrital in these rocks. One method suggested to determine if clay minerals are detrital or authigenic is to analyze clay crystallinity (e.g., Frey, 1987). Unfortunately, this analysis is generally not successful in fine-grained rocks. Clay crystallinity analysis assumes that the pore spaces of the rock are large enough for euhedral crystals to form. In fine-grained rocks, such as those in this study, it is impossible to differentiate between very small well-formed crystals and very small broken detrital bits (L. Williams, 1998, personal communication).

The effect of clay minerals on silica diagenesis in these two groups will be explored by examining the variation in the content of clay minerals on porosity reduction (Figure 4). The group 1 samples (Figure 4A) show an increase

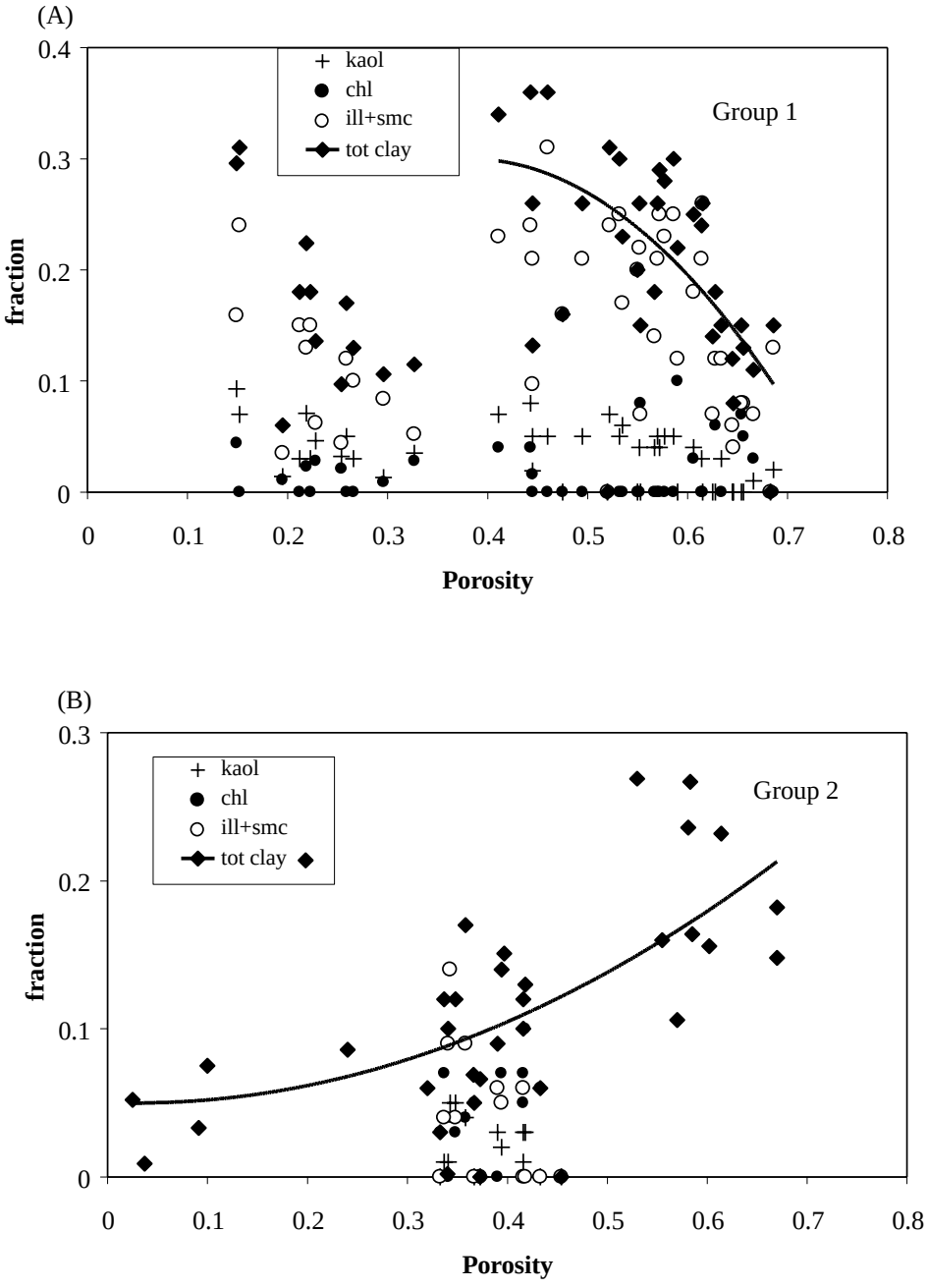

Figure 4—Fraction of clay minerals in the (A) group 1 and (B) group 2 samples vs. porosity. Regressions are calculated only for the samples where the diagenetic silica is primarily in the form of opal-A or opal-CT.

in clay through the opal-A/opal-CT transition and another increase through the opal-CT/quartz transition; furthermore, this change is primarily in illite and smectite minerals, which are more likely to be authigenic than chlorite, a low-grade metamorphic mineral (Zoltai and Stout, 1984). Clay crystallinity cannot be measured in these fine-grained rocks; however, with decreasing porosity, the increase in illite and smectite and relatively constant amount of chlorite suggests that the former is authigenic in origin.

In contrast, the group 2 samples show a decrease in clay minerals with decreasing porosity. Unfortunately, the clay mineralogy of the Point Pedernales minerals was not subdivided, and the McKittrick samples are fairly homogeneous; therefore, this analysis cannot be used to theorize

Table 1. Comparison of Group 1 and Group 2

Group 1	Group 2
Follows $\rho_b = 2.573 - 2.727\phi$, $R^2 = 0.995$	Follows $\rho_b = 2.7174 - 2.140\phi$, $R^2 = 0.949$
Grain density increases with decreasing porosity	Grain density decreases with decreasing porosity
Opal-A and opal-CT coexist at same porosity (often in same sample)	Opal-A and opal-CT seldom coexist at same porosity
Clay content increases with porosity reduction	Clay content does not increase with porosity reduction
Samples exist at continuous porosity	Porosity gap

whether the variation in clay minerals with porosity reduction in group 2 minerals is due to detrital variation or dissolution of clays with burial and diagenesis.

Although all available data on the percentages of clay minerals in these samples are shown in Figure 4, group 1 and group 2 can be compared only through the opal-A to opal-CT transition; therefore, regressions for the relationship between total clay minerals and porosity in samples where the diagenetic silica is predominantly opal-A and/or opal-CT are

$$\begin{aligned} &\text{Clay} = -0.019 + 1.67\phi - 2.19\phi^2 \\ &R^2 = 0.392 \\ &n = 32 \end{aligned} \tag{7}$$

for the group 1 samples, and

$$\begin{aligned} &\text{Clay} = 0.0500.021\phi + 0.39\phi^2 \\ &R^2 = 0.365 \\ &n = 34 \end{aligned} \tag{8}$$

for the group 2 samples. (In other words, the Asphalto samples and the one quartz-phase group 2 sample are removed from calculation of the regression equation.) The low correlation coefficient is not due to analyzing total clay rather than illite + smectite; the correlation coefficient does not increase if the latter is regressed for the group 1 samples. Because variations in clay mineralogy are caused by an array of variables, the low correlation coefficients are not unsurprising. It is more surprising that the correlation coefficients are so similar in both patterns. The role of clay minerals is of equal importance—yet opposite in magnitude—in estimating porosity in the two groups.

The positive relationship between clay and porosity in group 2 and the negative relationship in group 1 rocks is related to the primary porosity reduction mechanism in the two types of rocks. The group 1 rocks show a relationship where the abundance of clay minerals increases through the two diagenetic silica transition zones. Most of this increase is illite and smectite minerals, which are often authigenic in origin. Thus, these clay minerals form during diagenesis and reduce porosity by filling pore spaces. Because clays often clog pores and cause reduced porosity, it is unusual that in the group 2 samples, the more clay present the higher the porosity (Figure 4B); however, this observation is consistent with the fact that clays inhibit the formation of opal-CT, and the opal-A to opal-CT transition is the primary cause of porosity reduction in these samples.

PRACTICAL APPLICATIONS

The porosity of group 1 rocks containing opal-CT and diagenetic quartz-phase rocks is greater than generally documented. Isaacs (1981) data suggested that diagenetic quartz-phase rocks have a porosity of less than 20% and opal-CT–phase rocks have a porosity of less than 40%. The highest porosity quartz-bearing group 1 sample has a porosity of 26%, slightly larger than expected; however, there is a large difference in porosity between group 1 and group 2 opal-CT–phase rocks. Although the highest porosity opal-CT–phase group 2 sample in this study has porosity of 43%, group 1 samples containing primarily opal-CT have porosity as great as 65%. The significant difference between the pore volumes of group 1 and group 2 rocks, particularly opal-CT phase, has clear implications for the potential volume of stored hydrocarbons in Monterey Formation rocks.

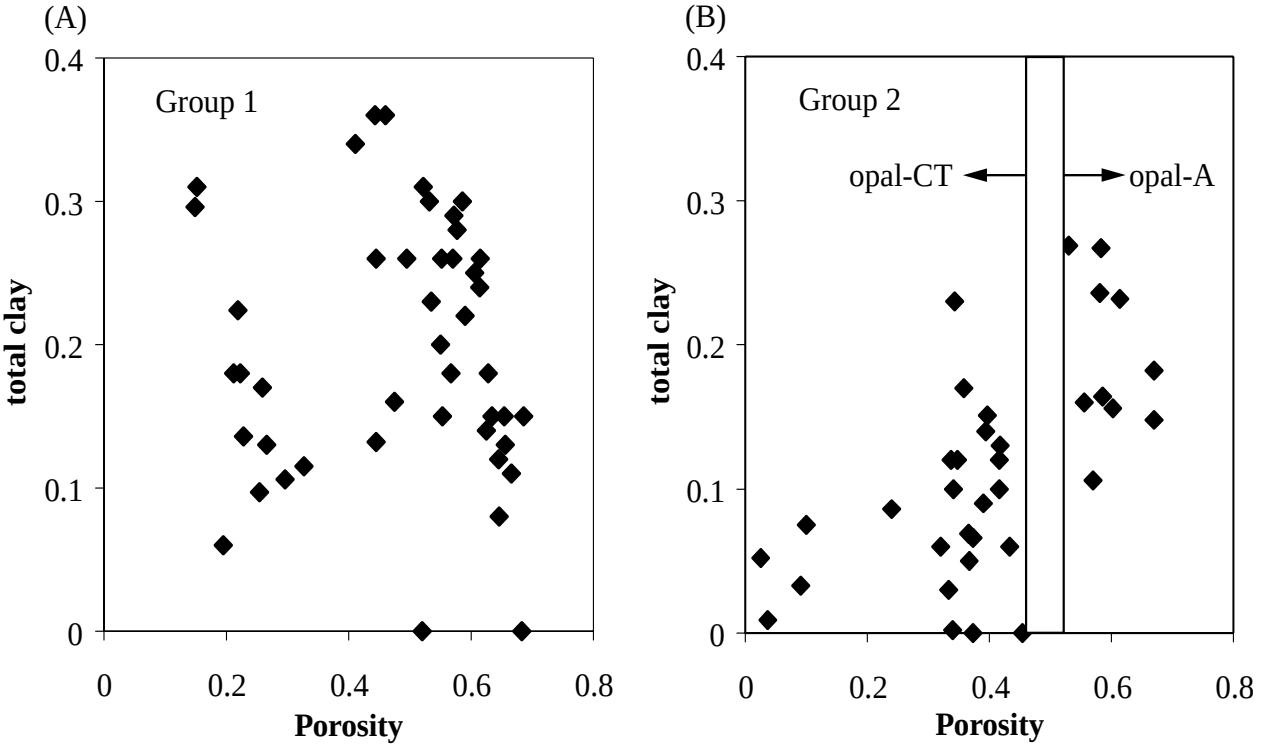

Figure 5—Fraction of total clay minerals in (A) group 1 and (B) group 2 samples.

CONCLUSIONS

Two different porosity reduction patterns exist in opaline rocks—one controlled by pore filling by clay minerals and one controlled by silica transformations.

In group 1, porosity decreases as the fraction of nonsilica minerals, such as clay minerals, increases. The clay minerals that increase with decreasing porosity are illite and smectite and likely formed during burial; therefore, porosity in group 1 rocks is reduced through pore filling by clay minerals.

The second pattern (group 2) has a sharp decrease in porosity through the opal-A/opal-CT transition marked by a porosity gap. Samples above 53% porosity contain opal-A, samples below 45% porosity contain opal-CT, and no samples occur within that interval. With decreasing porosity in group 2 samples, total content of silica minerals increases; therefore, as porosity decreases, the amount of clay minerals decreases and the grain density of samples decreases. Porosity reduction in these rocks appears to be controlled by the silica transformations. Because of this fact, opal-CT–bearing samples show the unusual trend where the content of clay minerals decreases with decreasing porosity.

The differences between the group 1 and group 2 samples are summarized in Table 1 and illustrated in Figure 5, which shows the data from Belridge, Cymric, and Asphalto on one side (group 1) and the data from Point Pedernales and McKittrick (group 2) on the other side. The first group (Figure 5A) shows a continuous reduction in porosity due to an increased content of clay minerals. The second group (Figure 5B) exhibits an abrupt porosity reduction from 53 to 45% due to the opal-A to opal-CT transition.

Porosity in the opal-CT–bearing samples of group 1 is larger than that of the opal-CT–bearing samples of group 2. Similarly, it is likely that group 1 samples with diagenetic quartz may have larger porosities than quartz-phase samples in group 2. These facts have significant implications for exploration in these important oil-bearing rocks.

APPENDIX

Sample Properties*

Group 1: Asphalto (well 332X-25Z, Sec. 25, T30S, R22E)

Depth (ft)	Phi	Gr Den	Opal-CT	Qtz	Alb	And	Ksp	Total Fsp	Kaol	Chl	Ill + Smc	Total Clay	Carb	Pyr	Org
5875	0.219	2.55	0	0.55	0.10	0	0.04	0.14	0.07	0.02	0.13	0.22	0	0.03	0.04
5876	0.266	2.53	0	0.70	0	0.06	0.09	0.15	0.03	0	0.10	0.13	0	0.02	0
5887	0.212	2.50	0	0.65	0.04	0.03	0.07	0.14	0.03	0	0.15	0.18	0.01	0.02	0
5892	0.223	2.52	0	0.67	0	0.04	0.08	0.12	0.03	0	0.15	0.18	0	0.03	0
5900	0.152	2.54	0	0.46	0.06	0.04	0.08	0.18	0.07	0	0.24	0.31	0.02	0.03	0
5914	0.149	2.54	0	0.42	0.10	0	0.06	0.16	0.09	0.04	0.16	0.30	0.04	0.03	0.04
5916	0.259	2.54	0	0.67	0.06	0.02	0.05	0.13	0.05	0	0.12	0.17	0	0.03	0
5931	0.327	2.56	0.15	0.57	0.06	0	0.03	0.09	0.04	0.03	0.05	0.12	0.02	0.02	0.04
5932	0.254	2.55	0.19	0.55	0.07	0	0.04	0.11	0.03	0.02	0.04	0.10	0.01	0.02	0.03
5937	0.195	2.43	0.46	0.36	0.06	0	0.02	0.08	0.01	0.01	0.04	0.06	0	0.01	0.02
5942	0.445	2.56	0.31	0.45	0.03	0	0	0.03	0.02	0.02	0.10	0.13	0.03	0.01	0.04
5957	0.228	2.54	0	0.66	0.08	0	0.04	0.12	0.05	0.03	0.06	0.14	0.01	0.02	0.04
5958	0.296	2.59	0.32	0.44	0.05	0	0	0.05	0.01	0.01	0.08	0.11	0.04	0.02	0.03

Group 1: North Belridge (SWEPI well 565S1, Sec. 1, T28S, R20E)

Depth (ft)	Phi	Gr Den	Opal-A	Opal-CT	Qtz	Alb	Ksp	And	Total Fsp	Kaol	Ill + Smc	Total Clay	Dolo	Pyr
1257	0.614	2.39	0.53	0	0.05	0.08	0.07	0.09	0.24	0.03	0.21	0.24	0.04	0.02
1301	0.475	2.52	0.21	0	0.20	0	0.11	0.19	0.30	0	0.16	0.16	0	0.02
1695	0.550	2.46	0.36	0	0.08	0	0.16	0.10	0.26	0	0.20	0.20	0	0.01
1745	0.615	2.38	0.49	0	0.09	0.09	0.08	0.08	0.25	0	0.26	0.26	0	0
1761	0.634	2.38	0.57	0	0.08	0	0.08	0.08	0.16	0.03	0.12	0.15	0	0.02
1796	0.552	2.44	0.42	0	0.12	0	0.07	0.07	0.14	0.04	0.22	0.26	0	0.02
1920	0.686	2.31	0.66	0	0.06	0	0.06	0.06	0.12	0.02	0.13	0.15	0	0
1975	0.535	2.40	0.33	0.21	0.07	0	0.06	0.06	0.12	0.06	0.17	0.23	0	0.01
2010	0.567	2.42	0	0.61	0.02	0	0.05	0.05	0.10	0.04	0.14	0.18	0	0.02
2107	0.495	2.46	0	0.47	0	0	0.11	0.11	0.22	0.05	0.21	0.26	0	0.03
2493	0.445	2.50	0	0.35	0.06	0.07	0.12	0.12	0.31	0.05	0.21	0.26	0	0.02

Group 1: South Belridge (Belridge V well 8360A-2, Sec. 2, T29S, R21E)

Depth (ft)	Phi	Gr Den	Opal-A	Opal-CT	Qtz	Alb	Ksp	And	Total Fsp	Kaol	Smc	Chl	Total Clay	Carb	Pyr
1694	0.577	2.32	0.44	0	0.08	0	0.12	0.04	0.16	0.05	0.23	0	0.28	0	0.04
1714	0.572	2.34	0.42	0	0.10	0	0.11	0.03	0.14	0.04	0.25	0	0.29	0	0.05
1820	0.460	2.43	0.32	0	0.09	0	0.11	0.06	0.17	0.05	0.31	0	0.36	0.03	0.03
1832	0.532	2.39	0.34	0	0.08	0	0.14	0.10	0.24	0.05	0.25	0	0.30	0	0.04
1836	0.586	2.35	0.36	0	0.09	0	0.14	0.08	0.22	0.05	0.25	0	0.30	0	0.03
1846	0.522	2.40	0.40	0	0.08	0	0.11	0.06	0.17	0.07	0.24	0	0.31	0.02	0.02
1882	0.606	2.27	0.36	0.21	0	0.04	0.07	0.05	0.16	0.04	0.18	0.03	0.25	0	0.02
1895	0.570	2.30	0.27	0.25	0.02	0.05	0.07	0.03	0.15	0.05	0.21	0	0.26	0.02	0.03
1906	0.443	2.31	0	0.41	0.04	0.06	0.09	0	0.15	0.08	0.24	0.04	0.36	0.02	0.02
1930	0.411	2.45	0.19	0.23	0	0.07	0.08	0.06	0.21	0.07	0.23	0.04	0.34	0	0.03

Group 1: Cymric Field (well 1407R-1Y, Sec. 1, T29S, R21E)

Depth (ft)	Phi	Gr Den	Opal-A	Opal-CT	Qtz	Alb	Ksp	And	Total Fsp	Kaol	Chl	Ill + Smc	Total Clay	Calc	Pyr	Anal
1240	0.520	2.27	0.42	0	0	0.06	0	0.10	0.16	0	0	0	0	0	0.01	0.41
1241	0.666	2.25	0.53	0.25	0.02	0	0.08	0	0.08	0.01	0.03	0.07	0.11	0	0.01	0
1243	0.625	2.37	0	0.74	0	0.08	0.04	0	0.12	0	0.07	0.07	0.14	0	0	0
1247	0.628	2.26	0.25	0.47	0	0.05	0.05	0	0.10	0	0.06	0.12	0.18	0	0	0
1249	0.656	2.33	0.41	0.36	0	0.06	0.04	0	0.10	0	0.05	0.08	0.13	0	0	0
1249	0.646	2.26	0.72	0.16	0	0	0.04	0	0.04	0	0.04	0.04	0.08	0	0	0
1249	0.683	2.21	0.57	0.28	0	0	0	0.05	0.05	0	0	0	0	0	0.01	0.09

Table Continued

Group 1: Cymric Field (well 1407R-1Y, Sec. 1, T29S, R21E)

Depth (ft)	Phi	Gr Den	Opal-A	Opal-CT	Qtz	Alb	Ksp	And	Total Fsp	Kaol	Chl	Ill + Smc	Total Clay	Calc	Pyr	Anal
1255	0.654	2.25	0	0.77	0	0.08	0	0	0.08	0	0.07	0.08	0.15	0	0	0
1256	0.645	2.25	0.23	0.49	0	0.07	0.07	0	0.14	0	0.06	0.06	0.12	0	0.02	0
1258	0.553	2.26	0	0.78	0	0.07	0	0	0.07	0	0.08	0.07	0.15	0	0	0
1259	0.590	2.29	0	0.64	0	0.10	0.03	0	0.13	0	0.10	0.12	0.22	0.01	0	0

Group 2: McKittrick Field (well 342-17Z, Sec. 17, T30S, R22E)

Depth (ft)	Phi	Gr Den	Opal-A	Opal-CT**	Qtz	Alb	Ksp	Olig	Total Fsp	Kaol	Smc	Chl	Total Clay	Calc	Pyr
3248.5	0.390	2.26	0	0.67	0	0	0.04	0.18	0.22	0.03	0.06	0	0.09	0	0.02
3255.5	0.454	2.20	0	0.88	0	0	0	0.12	0.12	0	0	0	0	0	0
3262.5	0.333	2.17	0	0.97	0	0	0	0	0	0	0	0.03	0.03	0	0
3268.5	0.373	2.34	0	0.95	0	0	0	0.05	0.05	0	0	0	0	0	0
3273.5	0.341	2.23	0	0.71	0	0	0.02	0.17	0.19	0.01	0.09	0	0.1	0	0
3306.0	0.348	2.24	0	0.71	0	0.10	0.05	0	0.15	0.05	0.04	0.03	0.12	0	0.02
3317.5	0.394	2.23	0	0.86	0	0	0	0	0	0.02	0.05	0.07	0.14	0	0
3337.5	0.367	2.18	0	0.95	0	0	0	0	0	0	0	0.05	0.05	0	0
3600.5	0.416	2.28	0	0.75	0	0	0.02	0.11	0.13	0.01	0.06	0.05	0.12	0	0
3603.5	0.433	2.24	0	0.9	0	0	0.04	0	0.04	0	0	0.06	0.06	0	0
3606.5	0.416	2.24	0	0.9	0	0	0	0	0	0.03	0	0.07	0.10	0	0
3670.5	0.337	2.25	0	0.83	0	0	0.05	0	0.05	0.01	0.04	0.07	0.12	0	0
3678.5	0.358	2.31	0	0.67	0	0.08	0.02	0.04	0.14	0.04	0.09	0.04	0.17	0.02	0
3681.0	0.343	2.30	0	0.65	0	0.12	0	0	0.12	0.05	0.14	0.04	0.23	0	0
3684.5	0.418	2.29	0	0.87	0	0	0	0	0	0.03	0	0.10	0.13	0	0

Group 2: Outcrop Data Collected Near Point Pedernales†

Depth (ft)	Phi	Gr Den	Opal-A	Opal-CT	Qtz	Alb	Ksp	And	Total Fsp	Kaol	Smc	Chl	Total Clay	Carb	Pyr
0.000	0.670	2.07	0.64	0	0.028				0.034				0.18	0.004	0.0030
360.9	0.581	2.23	0.41	0	0.073				0.17				0.24	0.004	0.0020
410.1	0.670	2.18	0.54	0	0.025				0.050				0.15	0.086	0.0050
524.9	0.583	2.21	0.40	0	0.057				0.13				0.27	0	0.0100
754.6	0.614	2.24	0.48	0	0.054				0.12				0.23	0.010	0.011
853.0	0.602	2.18	0.44	0	0.053				0.21				0.16	0.001	0.013
1246.7	0.585	2.27	0.41	0	0.068				0.20				0.16	0	0.0070
1476.4	0.530	2.18	0.35	0	0.068				0.096				0.27	0	0.0080
1574.8	0.025	2.01	0	0.73	0.037				0.10				0.052	0.002	0.0090
1656.8	0.570	2.08	0.37	0	0.083				0.24				0.11	0.006	0.012
1722.4	0.555	2.06	0.42	0	0.056				0.14				0.16	0.015	0.016
2066.9	0.397	2.19	0	0.50	0.058				0.14				0.15	0.003	0.024
2822.0	0.037	2.49	0	0.13	0.82				0.021				0.010	0	0.0020
2962.6	0.240	2.12	0	0.74	0.040				0.020				0.086	0	0.017
3274.3	0.320	2.21	0	0.40	0.050				0.074				0.060	0.240	0.040
3287.4	0.100	2.08	0	0.72	0.058				0.014				0.075	0	0.014
3330.1	0.091	1.95	0	0.75	0.11				0.049				0.033	0	0.0090
3494.1	0.373	2.21	0	0.53	0.032				0.054				0.066	0.22	0.014
3838.6	0.366	2.12	0	0.72	0.037				0.092				0.069	0	0.018
3920.6	0.340	2.06	0	0.76	0.037				0.071				0.002	0.022	0.019

*Phi = porosity, gr den = grain density, qtz = quartz, alb = albite, ksp = orthoclase feldspar, and = andesine, total fsp = total feldspar, kao = kaolinite, ill+smc = illite+ smectite, chl = chlorite, calc = calcite, dolo = dolomite, carb = dolomite + calcite, pyr = pyrite, anal = analcime, org = organic material.

**Opal-CT = Opal-CT+ cristobalite; trace minerals include < 0.01 apatite + halite.

†Compton (1991).

REFERENCES CITED

Beyer, L. A., 1987, Porosity of unconsolidated sand, diatomite, and fractured shale reservoirs, South Belridge and West Cat Canyon oil fields, California, *in* R. F. Meyer, ed., Exploration for heavy crude oil and natural bitumen: AAPG Studies in Geology 25, p. 395–413.

Carmichael, R. S., 1989, Practical handbook of physical properties of rocks and minerals: Boca Raton, Florida, CRC Press, 741 p.

Chaika, C. J., 1998, Physical properties and silica diagenesis: Ph.D. dissertation: Stanford University, Stanford, California, 117 p.

Compton, J. S., 1991, Porosity reduction and burial history of siliceous rocks from the Monterey and Sisquoc Formations, Point Pedernales area, California: Geological Society of America Bulletin, v. 103, p. 625–636.

Dove, P. M., and J. D. Rimstidt, 1994, Silica-water interactions, *in* P. J. Heaney, C. T. Prewitt, and G. V. Gibbs, eds., Silica: physical behavior, geochemistry, and materials applications: Mineralogical Society of America, Reviews in Mineralogy, v. 29, p. 259–308.

Frey, M., 1987, Very low-grade metamorphism of clastic sedimentary rocks, *in* M. Frey, ed., Low temperature metamorphism: New York, Chapman and Hall, p. 9–58.

Graetsch, H., 1994, Structural characteristics of opaline and microcrystalline silica minerals, *in* P. J. Heaney, C. T. Prewitt, and G. V. Gibbs, eds., Silica: physical behavior, geochemistry and materials applications: Mineralogical Society of America, Reviews in Mineralogy, v. 29, p. 209–232.

Guerin, G., and D. Goldberg, 1996, Acoustic and elastic properties of calcareous sediments across a siliceous diagenetic front on the eastern U.S. continental slope: Geophysical Research Letters, v. 23, p. 2697–2700.

Harville, D. G., and D. L. Freeman, 1988, The benefits of application of rapid mineral analysis provided by Fourier transform infrared spectroscopy: SPE Conference Proceedings, p. 141–146.

Hinman, N. W., 1990, Chemical factors influencing the rates and sequences of silica phase transitions: effects of organic constituents: Geochimica et Cosmochimica Acta, v. 54, p. 1563–1574.

Isaacs, C. M., 1981, Porosity reduction during diagenesis of the Monterey Formation, Santa Barbara coastal area, California, *in* R. E. Garrison and R. G. Douglas, eds., The Monterey Formation and related siliceous rocks of California: SEPM Pacific Section, p. 257–271.

Isaacs, C. M., 1983, Compositional variation and sequence in the Miocene Monterey Formation, Santa Barbara coastal area, California, *in* D. K. Larue and R. J. Steel, eds., Cenozoic marine sedimentation, Pacific margin, U.S.A.: SEPM Pacific Section, p. 117–132.

Kastner, M., J. B. Keene, and J. M. Gieskes, 1977, Diagenesis of siliceous oozes—I. Chemical controls on the rate of opal-A to opal-CT transformation—an experimental study: Geochimica et Cosmochimica Acta, v. 41, p. 1041–1059.

Merino, E., 1975, Diagenesis in Tertiary sandstones from Kettleman North dome, California, I. Diagenetic mineralogy: Journal of Sedimentary Petrology, v. 45, no. 1, p. 320–336.

Murata, K. J., and R. R. Larson, 1975, Diagenesis of Miocene siliceous shales, Temblor Range, California: U.S. Geological Survey Journal of Research, v. 3, p. 553–566.

Murata, K. J., and R. G. Randall, 1975, Silica mineralogy and structure of the Monterey Shale, Temblor Range, California: U.S. Geological Survey Journal of Research, v. 3, p. 567–572.

Nobes, D. C., R. W. Murray, S. Kuramoto, K. A. Pisciotto, and P. Holler, 1992, I. Impact of silica diagenesis on physical property variations, *in* K. A. Pisciotto, J. C. Ingle, Jr., M. T. von Breymann, and J. Barron, eds., Proceedings of the ODP scientific results, part I: Washington, D. C., NSF and Joint Oceanographic Institutions, v. 127, p. 3–32.

O'Brien, D. K., M. H. Manghnani, and J. S. Tribble, 1989, Irregular trends of physical properties in homogeneous clay-rich sediments of DSDP Leg 87 Hole 584, Midslope terrace in the Japan Trench: Marine Geology, v. 87, p. 183–194.

Pisciotto, K. A., 1981, Diagenetic trends in the siliceous facies of the Monterey Shale in the Santa Maria region, California: Sedimentology, v. 28, p. 547–571.

Rice, S. B., H. Freund, W.-L. Huang, J. A. Clouse, and C. M. Isaacs, 1995, Application of Fourier Transform infrared spectroscopy to silica diagenesis: Journal of Sedimentary Petrology, v. A65, no. 4, p. 639–647.

Rimstidt, J. D., and H. L. Barnes, 1980, The kinetics of silica-water reactions: Geochimica et Cosmochimica Acta, v. 44, p. 1683–1699.

Schwartz, D. E., 1988, Characterizing the lithology, petrophysical properties, and depositional setting of the Belridge diatomite, South Belridge field, Kern County, California, *in* S. A. Graham, ed. Studies of the geology of the San Joaquin basin: SEPM Pacific Section, v. 60, p. 281–301.

Tada, R., and A. Iijima, 1983, Petrology and diagenetic changes of Neogene siliceous rocks in northern Japan: Journal of Sedimentary Petrology, v. 53, no. 3, p. 911–930.

Tribble, J. S., F. T. Mackenzie, J. Urmos, D. K. O'Brien, and M. H. Manghnani, 1992, Effects of biogenic silica on acoustic and physical properties of clay-rich marine sediments: AAPG Bulletin, v. 76, no. 6, p. 792–804.

Williams, L. A., and D. A. Crerar, 1985, Silica diagenesis II. General mechanisms: Journal of Sedimentary Petrology, v. 55, no. 3, p. 312–321.

Williams, L. A., G. A. Parks, and D. A. Crerar, 1985, Silica diagenesis I. Solubility controls: Journal of Sedimentary Petrology, v. 55, no. 3, p. 301–311.

Zoltai, T., and J. H. Stout, 1984, Mineralogy: concepts and principles: Minneapolis, Minnesota, Burgess Publishing Company, 505 p.

ABOUT THE AUTHORS

Caren Chaika

Caren Chaika is currently a geologist at Occidental of Elk Hills located outside of Bakersfield, California. She received her B.A. degree in geology from Rice University in 1993. In 1998, she received her Ph.D. in the Department of Geological and Environmental Sciences at Stanford University, where she combined geology and rock physics to explore the effect of diagenesis on the mechanical and storage properties of rocks.

Jack Dvorkin

Jack Dvorkin holds a Ph.D. in mechanics and mathematics (1980) from Moscow University. He is currently a senior research scientist at the Geophysics Department of Stanford University. His main interest is in rock physics reservoir characterization. He is a founder of Petrosoft, Inc., and Petrophysical Consulting, Inc., where he serves as general manager. He is the author of about 70 journal publications and two books.